Design Study for HybriSCU: A HYBRID NbTi/ReBCO Superconducting Undulator

V. Grattoni and S. Casalbuoni

Abstract—At the European XFEL, the undulator systems group has started in 2020 an R&D project dedicated to the development of innovative superconducting undulator (SCU) coils. SCUs are of great interest for storage rings and free electron lasers (FEL) facilities as they enable to widen the tunability range of the generated photon energy for the same electron beam energy compared with the established technology of the permanent magnet undulators. In this contribution, we present the characterization study and the achievable performance of HybriSCU a graded SCU coil combining two different superconductors: NbTi and high temperature superconductor (HTS) based on Rare-Earth Barium Copper Oxide (ReBCO) tape.

Index Terms—Superconducting undulator, HTS, accelerator magnets.

I. INTRODUCTION

UNDULATORS are devices with a periodic magnetic structure, which allows them to generate a sinusoidal magnetic field. Planar undulators consist of two symmetric arrays facing each other. The distance in between is called the magnetic gap. The light sources based on electron accelerators exploit undulators to generate highly collimated and intense photon beams.

When an electron beam advances through the undulator, it emits radiation at wavelengths:

$$\lambda_n = \frac{\lambda_u}{2n\gamma^2}\left(1 + \frac{K^2}{2} + \gamma^2\theta^2\right) \tag{1}$$

where n is the harmonic number, λ_u is the period length of the undulator, γ is the Lorentz factor of the electron beam, $K \simeq 93.4 B_0[T]\lambda_u[m]$ is the undulator parameter with B_0 the peak of the magnetic field on axis where the electron is travelling, and θ is the angle at which an observer is looking at the generated radiation. The strength of the magnetic field on axis depends on the magnetic gap, the period of the undulator and the undulator technology itself [1].

Experimental measurements show that superconducting undulators (SCUs) based on Niobium-Titanium (NbTi) have a higher peak field on axis for the same gap and period length compared to permanent magnet undulators, and also in-vacuum undulators or cryogenic permanent magnet undulators [2], [3]. As a consequence, also the undulator parameter K of the SCUs is higher and therefore the tunability range of the generated radiation wavelength is larger compared to other technologies.

The undulator parameter K can be further increased in SCUs with the period doubling scheme [4].

In this contribution, HybriSCU is introduced as a hybrid SCU that utilizes both NbTi wire and Rare-Earth Barium Copper Oxide (ReBCO) tape.

High-Temperature Superconductors (HTS) based on ReBCO tape offer the possibility of operating at higher temperatures than NbTi and have a higher critical current when operated at low temperatures ($4.2\,\mathrm{K}$ or $2.2\,\mathrm{K}$). In recent years, various schemes using ReBCO tape have been explored. The patent [5] in 2012 has shown the first possible scheme for the realization of a planar undulator based on ReBCO tape with splices. The undulator was also characterized at CASPAR1 at KIT [6]. A few years later, a continuous winding planar coil was tested successfully in [7], demonstrating a 40% higher engineering current density than the NbTi-based undulator. The concept of a Meander structured stacked ReBCO tape undulator was initially proposed in [8]. Later, a jointless scheme was implemented at KIT, as reported in [9]. Additionally, staggered-array bulk HTS planar undulators were realized using ReBCO bulks. The latest results achieved a peak field on axis of $1.54\,\mathrm{T}$ at $10\,\mathrm{K}$ with a $4\,\mathrm{mm}$ magnetic gap, as reported in [10]. For a comprehensive review of the most recent tests on ReBCO-based undulators, the authors suggest referring to [11].

HybriSCU surpasses the performances of the NbTi-based SCU in terms of magnetic field on axis further enhancing its tunability range. HybriSCU is a graded undulator that uses both NbTi and ReBCO tape. Graded magnets are commonly used in various applications, such as high-field solenoids for NMR and laboratory use, as well as dipoles for particle accelerators like high-energy colliders, where a high magnetic field is necessary. These magnets often combine NbTi, Nb_3Sn, and ReBCO materials to achieve the desired field strength and other performance characteristics, as reported in several studies [12], [13], [14], [15].

ReBCO tapes are commercially available in lengths up to about $100\,\mathrm{m}$. Thus, an SCU based only on ReBCO tape cannot be realized without resistive joints yet. Moreover, ReBCO tapes are about 10 times more expensive than NbTi wire. As a result, the design is based on a graded SCU. HybriSCU is wound with
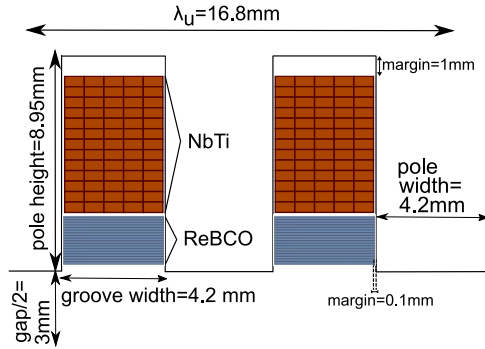
Fig. 1.　Main dimensions of HybriSCU.

Fig. 2.　Loadline of an SCU with only 15 layers of NbTi and following the geometry from Fig. 1.

NbTi wire at the bottom of the grooves and with a few layers of ReBCO tape in the region close to the electron beam. This allows us to take advantage of the high current density and large temperature margin of the ReBCO tape.

In the first section, the geometry of HybriSCU is presented. In the second section, the calculation of the critical curves for NbTi and ReBCO is described. The third section presents a comparison of HybriSCU in terms of performance against SCUs with the same geometry based on either only NbTi or only ReBCO. Finally, the conclusions of the study are presented.

II. MAIN PARAMETERS FOR HYBRISCU

HybriSCU was designed based on the geometry of commercially available ReBCO tape, and the period was defined to be as short as possible while still allowing for the ReBCO tape to be wound with its largest surface parallel to the bottom face of the grooves. The tape width is offered in a few discrete options by companies. The most common tape width is $12\,\mathrm{mm}$ and companies like SuperOX and Superpower offer also the width assumed for this study $4\,\mathrm{mm}$. The pole and the groove width are set to $4.2\,\mathrm{mm}$, resulting in an undulator period of $16.8\,\mathrm{mm}$. The groove accommodates one turn of the ReBCO tape and accounts for a margin of $0.1\,\mathrm{mm}$ plus insulation with Kapton foil. Considering a NbTi rectangular wire with dimension $0.8\,\mathrm{mm}$ width and $0.5\,\mathrm{mm}$ height, a groove can be filled with 5 turns and 15 layers. A gap of $1\,\mathrm{mm}$ in height is maintained at the bottom of the groove to prevent excessive high fields on the NbTi, along with a margin of $0.2\,\mathrm{mm}$ in height to account for mechanical tolerances. Additional $0.25\,\mathrm{mm}$ are left free on top of the groove (close to the vacuum beam pipe) for possible shimming coils. This results in a groove height of $8.95\,\mathrm{mm}$. The main dimensions of HybriSCU are specified in Fig. 1.

In the HybriSCU design, a portion of the NbTi layers is substituted with ReBCO tape. A tape that does not contain a stabilizer, but instead features two silver layers that encase the substrate, buffer stack, and ReBCO layer, with a total thickness of $30\,\mathrm{\mu m}$ is utilized, as described by SuperPower [16]. To ensure proper passage to the consecutive groove, an odd number of NbTi layers are always maintained.
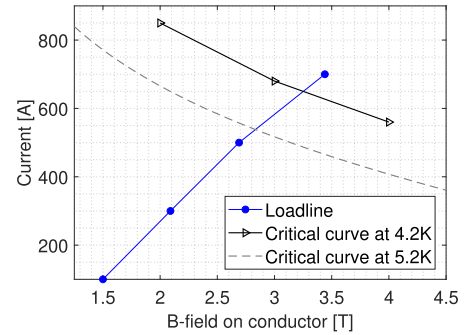
III. CRITICAL CURVES

In this study, an operational temperature of $4.2\,\mathrm{K}$ is being considered for HybriSCU. The operating current in the NbTi is determined by setting it as the current at the point of intersection between the loadline and the critical current at $5.2\,\mathrm{K}$, considering $1\,\mathrm{K}$ margin from the operating temperature. Fig. 2 shows the loadline of the NbTi and the critical current curves at various temperatures. The measured critical current data of the NbTi wire at $4.2\,\mathrm{K}$ is scaled to obtain the current at $1\,\mathrm{K}$. The critical current is calculated using the scaling law defined in [17]:

$$I_C(B,T) = I_{C,ref} \frac{C}{B} \left(\frac{B}{B_{C2}(T)} \right)^\alpha \left(1 - \frac{B}{B_{C2}(T)} \right)^\beta$$
$$\times \left[1 - \left(\frac{T}{T_{C0}} \right)^{1.7} \right]^\gamma$$

where $I_{C,ref} = 610\,\mathrm{A}$ is the wire critical current at $4.2\,\mathrm{K}$, $C = 27.4\,\mathrm{T}$, $\alpha = 0.68$, $\beta = 0.8$, $\gamma = 2.74$ are the fitting parameters typical for NbTi, $T_{C0} = 9.2\,\mathrm{K}$ is the critical temperature at zero magnetic field and $B_{C2}(T)$ is the peak field for the NbTi:

$$B_{C2}(T) = B_{C20} \cdot \left[1 - \left(\frac{T}{T_{C0}} \right)^{1.7} \right] \qquad (2)$$

with the upper critical field at $0\,\mathrm{K}$, $B_{C20} = 14.5\,\mathrm{T}$.

The determination of the critical current of the ReBCO tape is more complex compared to low-temperature superconductors like NbTi. The critical current of the ReBCO tapes not only depends on the temperature and the applied magnetic field but also on the orientation of the magnetic field against the tape surfaces. In addition, the ReBCO tapes behave differently depending on the deposition method exploited to apply the superconductor on the substrate and the critical current varies from batch to batch of the same producer. As a result, experimental characterization of every batch would be needed. The available measurement systems to characterize such tapes present limitations depending on the setup like minimum temperature that can be achieved [18], field angle [19], maximum applied field [20] or maximum applied current. For this study, a second-generation tape with advanced pinning from Superpower [16] is considered, which behaves similarly to the tape from Superpower measured by the Robinson Research Institute (in New Zealand)

in the high-temperature superconducting wire critical current database [21]. The positive effect of advanced pinning is that it provides larger current densities. The vendors of ReBCO tapes are only providing the value of the critical current in the self-field at 77 K. A self-field critical current of $I_{C,T=77\,\mathrm{K},B=0\,\mathrm{T}}^{\mathrm{HybriSCU}} = 167\,\mathrm{A}$ at 77 K is being considered for the tape under investigation. Given the properties of the ReBCO tapes, a larger temperature margin has been chosen compared to the one assumed for the NbTi wire, using its larger tolerance to higher temperatures. A temperature margin of 11 K is selected for the ReBCO tape. As a result, the critical current at 15 K is being examined when operating at 4.2 K. The Superpower ReBCO tape currently under consideration contains nanosized columns of Barium zirconate (BZO) oriented along the c-axis. This design modification is intended to alter the pinning landscape and enhance the electrical transport properties of the tape. As a consequence, the angular dependence of the current density varies with the temperature for fields below 10 T [22]. In this contribution, we always take the value of the angle which gives the minimum critical current at a fixed temperature. The Superpower tape from the Robinson database [21] has a different critical current in the self field at 77 K $I_{C,T=77\,\mathrm{K},B=0\,\mathrm{T}}^{\mathrm{RD}}$.

Thus, to find the critical current in the self-field at 15 K for HybriSCU, we have to rescale the curve from the Robinson database (RD) with respect to the current $I_{C,T=77\,\mathrm{K},B=0\,\mathrm{T}}^{\mathrm{HybriSCU}}$. To do so, we find the following dependence of the critical current in self-field as a function of the temperature:

$$I_{C,B=0\,\mathrm{T}}^{\mathrm{HybriSCU}}(T) = \frac{I_{C,T=77\,\mathrm{K},B=0\,\mathrm{T}}^{\mathrm{HybriSCU}}}{I_{C,T=77\,\mathrm{K},B=0\,\mathrm{T}}^{\mathrm{RD}}} I_{C,B=0\,\mathrm{T}}^{\mathrm{RD}}(T). \quad (3)$$

The current in self-field at 15 K $I_{C,T=15\,\mathrm{K},B=0\,\mathrm{T}}^{\mathrm{HybriSCU}}$ results 1898 A for a tape with 4 mm width as the one for HybriSCU. The critical current at 15 K for HybriSCU is scaled from the Robinson database:

$$I_{C,T=15\,\mathrm{K}}^{\mathrm{HybriSCU}}(B) = \frac{I_{C,T=15\,\mathrm{K},B=0\,\mathrm{T}}^{\mathrm{HybriSCU}}}{I_{C,T=15\,\mathrm{K},B=0\,\mathrm{T}}^{\mathrm{RD}}} I_{C,T=15\,\mathrm{K}}^{\mathrm{RD}}(B) \quad (4)$$

Fig. 3 shows the calculated critical current for the ReBCO tape at 15 K and for reference, we have also added the critical current at 4 K that was provided by the company SuperPower for a similar ReBCO tape. We have not used this curve for the rescaling to find the critical current because we do not have the information of the current in the self field at 4 K. The same figure shows the loadlines for an undulator with grooves filled only with ReBCO tape and the different lines represent a different amount of layers: 7, 30, 60 and 90. The maximum field on axis is achieved with 60 layers of ReBCO reaching 2.7 T.

IV. HYBRISCU PERFORMANCE

Four configurations for HybriSCU have been considered: with 15, 13, 11 and 9 layers of NbTi and 7, 30, 60 and 90 layers of ReBCO, respectively. The height of the complete winding package is kept constant because the number of layers of ReBCO tape is related to the number of removed layers of NbTi wire, apart from the case with 7 layers of ReBCO. In this last case, the 15 layers of NbTi are kept and the 7 layers of ReBCO are placed above. In each case, different current configurations in
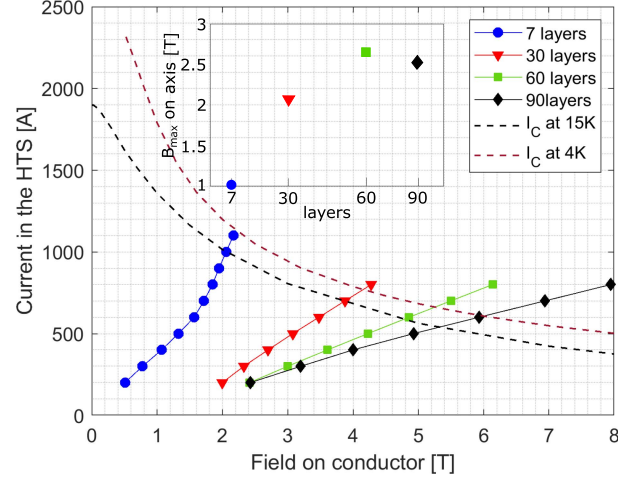

Fig. 3. Loadline for the SCU with only HTS and different layers: 7, 30, and 60. The inlet shows the maximum field on axis generated by these configurations.
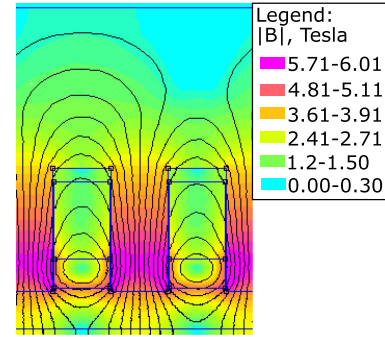

Fig. 4. Field lines from FEMM simulation for HybriSCU configuration with 13 layers of NbTi and 30 layers of ReBCO.

TABLE I
HYBRISCU COMPARED WITH ONLY NBTI AND ONLY REBCO LAYOUTS

Number of layers		Currents		B_{max} [T]
NbTi	ReBCO	I_{NbTi} [A]	I_{ReBCO} [A]	
15	—	540	—	1.610
15	7	540	700	1.911
13	30	470	630	2.456
11	60	400	559	2.816
—	60	—	600	2.670
9	90	340	529	3.060

the ReBCO and the NbTi were simulated using FEMM [23]. Fig. 4 shows the field lines on the conductors and on the poles of HybriSCU in the configuration with 13 layers of NbTi and 30 layers of HTS.

Table I summarizes the maximum field on axis achieved for the optimized HybriSCU configurations considering 1 K and 11 K margin for respectively NbTi and the ReBCO. Table I indicates that NbTi and ReBCO are operated with different current values, which necessitates the use of two power supplies to operate HybriSCU.

The procedure to find the current for the two conductors and derive the maximum field on axis of HybriSCU for the case with 13 layers of NbTi and 30 layers of ReBCO is described. The same procedure applies to the other configurations. Several
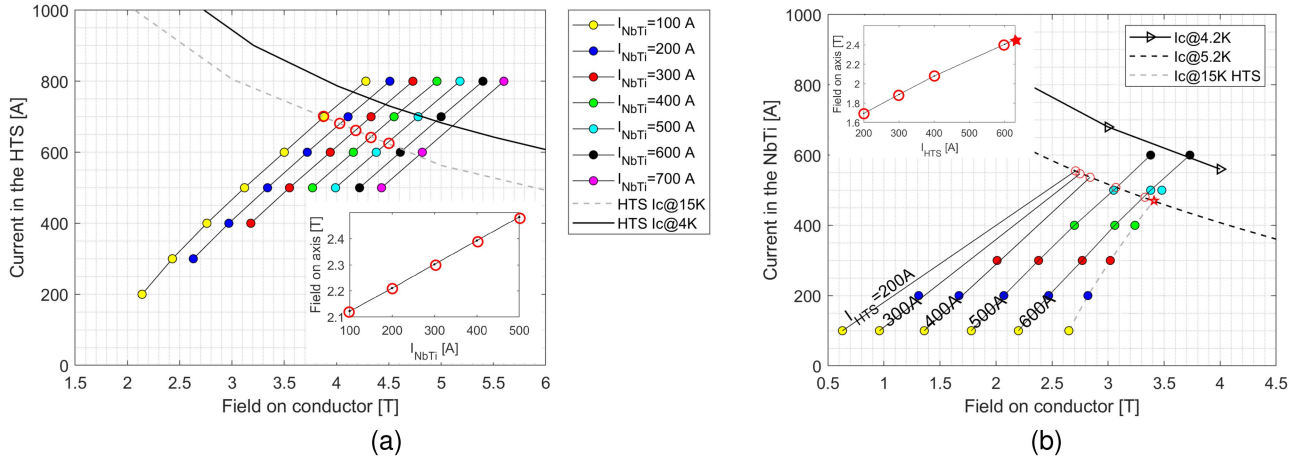
Fig. 5.   Loadline for the ReBCO tape (a) and the NbTi (b) for the HybriSCU with 13 layers of NbTi and 30 layers of ReBCO.

simulations of HybriSCU with different currents in the NbTi and the ReBCO have been performed to derive the loadlines. The greater current is always set in the ReBCO, as it has a higher critical current at $4.2 \, \mathrm{K}$ compared to the NbTi. The minimum current difference between the ReBCO and the NbTi is of $100 \, \mathrm{A}$. The field on both conductors was analyzed in every simulation. The resulting loadline for the ReBCO tape is shown in Fig. 5(a) and for the NbTi in Fig. 5(b). The dots represent the simulated points. The loadline for the ReBCO is considered first. Here, the current allowed in the ReBCO tape is extracted from the intersection point between the loadline and the critical current at $15 \, \mathrm{K}$. The parallel lines in Fig. 5(a) represent different currents in the NbTi. The maximum field on axis for a fixed current in the NbTi is achieved when the current in the ReBCO sits on the curve at $15 \, \mathrm{K}$. Therefore, for these points the values of the magnetic field on axis are registered. The inlet of Fig. 5(a) shows the field generated on axis. The peak field on axis increases by 25% as the current in the NbTi grows from $100 \, \mathrm{A}$ to $500 \, \mathrm{A}$. For higher currents in the NbTi, there are no more working points below the critical current at $15 \, \mathrm{K}$ of the ReBCO.

Fig. 5(b) shows the loadline for the NbTi given by the working points below and on the critical current of the ReBCO at $15 \, \mathrm{K}$. The points sitting on the critical current at $15 \, \mathrm{K}$ curve of the ReBCO are connected with a grey-dashed line. This line gives the maximum current in the ReBCO that can be set for each fixed current in the NbTi. The maximum current for the NbTi for a fixed current in the ReBCO, corresponds to the value coming from the intersection points between the NbTi loadline for a fixed current in the ReBCO and the critical curve of the NbTi at $5.2 \, \mathrm{K}$. The simulations show that the maximum peak field on axis increases by 30% as the current in the ReBCO is rising from $200 \, \mathrm{A}$ to $630 \, \mathrm{A}$. The maximum peak field on axis is achieved for a current of $630 \, \mathrm{A}$ in the ReBCO and $470 \, \mathrm{A}$ in the NbTi and it is shown as a star in the inlet of Fig. 5(b).

The same reasoning has been followed for the other configurations of HybriSCU. The final results of current in the conductors and maximum field on axis are reported in Table I. The slope of the ReBCO loadlines, and therefore the maximum current allowed in the ReBCO, is inversely proportional to the number of layers of ReBCO.

Table I shows the working points of HybriSCU for the different configurations of layers of the conductor. In this table, the performance of HybriSCU, in terms of the maximum field on axis, is compared with respect to an SCU with only 15 NbTi layers. All the HybriSCU configurations are improving the performance of the SCU with only NbTi, which gives a field on axis of $1.61 \, \mathrm{T}$. HybriSCU already improves by 15% the performance of the NbTi-based SCU by only adding 7 layers of ReBCO. Table I also shows the performance of HybriSCU against an SCU based on only 60 layers of ReBCO tape. The amount of ReBCO tape needed to realize HybriSCU with 9/90 layers of NbTi/ReBCO is not competitive, from the point of view of the cost and the needed length of tape. The authors consider advantageous the configurations with 15 or 13 layers of NbTi and 7 or 30 layers of ReBCO tape, with a maximum field on axis of $1.911 \, \mathrm{T}$ and $2.456 \, \mathrm{T}$ respectively.

V. CONCLUSION AND OUTLOOK

This contribution presents an innovative concept of a Hybrid Superconducting Undulator composed of two types of conductor: NbTi wire and ReBCO tape. The geometry, the performance of the device and the properties of the superconductors exploited has been described. The authors have concluded that the most advantageous configuration to enhance the performance of the current SCUs based on only NbTi would be to add just a few layers of ReBCO tape. HybriSCU with 15/7 layers of NbTi/ReBCO, the magnetic field on axis is 15% higher compared to the NbTi SCU with only 15 layers. The HybriSCU with 30 layers of ReBCO and 13 layers of NbTi has a peak field on axis that is 34% greater than the one of the NbTi-SCU and it costs 37% less than an ReBCO-SCU. Even if increasing the number of ReBCO layers above 30 is not convenient for cost reasons, we can still achieve an increase in peak field on axis of 5% and 17% for HybriSCU with respectively 60 and 90 layers of HTS with respect to an SCU based on only ReBCO tape.

Based on this study, the authors foresee to investigate the realization process of HybriSCU. Technical details like the electrical insulation between NbTi and the ReBCO and the passage of the ReBCO tape from one groove to the next one will be addressed.

REFERENCES

[1] P. Elleaume, J. Chavanne, and B. Faatz, "Design considerations for a 1Å sase undulator," *Nucl. Instrum. Methods Phys. Res. Sect. A: Accel., Spectrometers, Detect. Assoc. Equip.*, vol. 455, pp. 503–523, 2000.

[2] S. Casalbuoni et al., "Commissioning of a full scale superconducting undulator with 20 mm period length at the storage ring KARA," *AIP Conf. Proc.*, vol. 2054, no. 1, 2019, Art. no. 030025, doi: 10.1063/1.5084588.

[3] Y. Ivanyushenkov et al., "Development and operating experience of a short-period superconducting undulator at the advanced photon source," *Phys. Rev. ST Accel. Beams*, vol. 18, Apr. 2015, Art. no. 040703, doi: 10.1103/PhysRevSTAB.18.040703.

[4] S. Casalbuoni, N. Glamann, A. W. Grau, T. Holubek, and D. S. de Jauregui, "Superconducting undulator coils with period length doubling," *J. Phys.: Conf. Ser.*, vol. 1350, no. 1, Nov. 2019, Art. no. 012024, doi: 10.1088/1742-6596/1350/1/012024.

[5] C. Boffo and T. Gerhard, "High-temperature superconductor magnet system," German patent WO/2012/013205, U.S. Patent 8,849,364, pp. 1–20, Feb. 2012. [Online]. Available: https://patentimages.storage.googleapis.com/06/0d/3c/1d84048c62ecf6/WO2012013205A1.pdf

[6] S. Casalbuoni, "Superconducting undulators: Experience from ANKA," 2014. [Online]. Available: https://indico.psi.ch/event/3033/contributions/5249/attachments/4616/5727/Casalbuoni_BeMa2014.pdf

[7] I. Kesgin, M. Kasa, Y. Ivanyushenkov, and U. Welp, "High-temperature superconducting undulator magnets," *Supercond. Sci. Technol.*, vol. 30, no. 4, Feb. 2017, Art. no. 04LT01, doi: 10.1088/1361-6668/aa5d48.

[8] S. Prestemon, D. Dietderich, A. Madur, S. Marks, and D. Schlueter, "High performance short-period undulators using high temperature superconductor tapes," in *Proc. 23rd Part. Accel. Conf.*, Vancouver, BC, Canada, 2009, pp. 2438–2440. [Online]. Available: https://epaper.kek.jp/PAC2009/papers/we5rfp075.pdf

[9] T. Holubek et al., "A novel concept of high temperature superconducting undulator," *Supercond. Sci. Technol.*, vol. 30, no. 11, Sep. 2017, Art. no. 115002, doi: 10.1088/1361-6668/aa87f1.

[10] M. Calvi, "HTS undulators," in *Proc. Virtual Superconducting Undulators Adv. Light Sources Workshop*, 2021, pp. 27–44.

[11] K. Zhang and M. Calvi, "Review and prospects of world-wide superconducting undulator development for synchrotrons and FELs," *Supercond. Sci. Technol.*, vol. 35, no. 9, Jul. 2022, Art. no. 093001, doi: 10.1088/1361-6668/ac782a.

[12] L. Cavallucci, M. Breschi, P. L. Ribani, A. V. Gavrilin, H. W. Weijers, and P. D. Noyes, "A numerical study of quench in the NHMFL 32 T magnet," *IEEE Trans. Appl. Supercond.*, vol. 29, no. 5, Aug. 2019, Art. no. 4701605.

[13] J. Jaroszynski, "A new no-insulation REBCO magnet of 32 T class," *Supercond. Sci. Technol.*, vol. 33, no. 8, Jun. 2020, Art. no. 080501, doi: 10.1088/1361-6668/ab9686.

[14] R. Gupta et al., "Hybrid high-field cosine-theta accelerator magnet R&D with second-generation HTS," *IEEE Trans. Appl. Supercond.*, vol. 25, no. 3, Jun. 2015, Art. no. 4003704.

[15] R. Gupta et al., "Design, construction, and test of HTS/LTS hybrid dipole," *IEEE Trans. Appl. Supercond.*, vol. 28, no. 3, Apr. 2018, Art. no. 4002305.

[16] SuperPower, "2G HTS wire specification," 2022. [Online]. Available: https://www.superpower-inc.com/specification.aspx

[17] L. Bottura, "A practical fit for the critical surface of NbTi," *IEEE Trans. Appl. Supercond.*, vol. 10, no. 1, pp. 1054–1057, Mar. 2000.

[18] N. Strickland, C. Hoffmann, and S. Wimbush, "A 1 kA-class cryogen-free critical current characterization system for superconducting coated conductors," *Rev. Sci. Instrum.*, vol. 85, 2014, Art. no. 113907.

[19] C. Barth, M. Bonura, and C. Senatore, "High current probe for Ic(B,T) measurements with ±0.01 K precision: HTS current leads and active temperature stabilization system," *IEEE Trans. Appl. Supercond.*, vol. 28, no. 4, Jun. 2018, Art. no. 9500206.

[20] A.-H. Bergen, "Conduction-cooled REBCO coils for the wind converter: From laboratory to field test," Ph.D. dissertation, Univ. Twente, The Netherlands, Dec. 2020.

[21] S. Wimbush, "The robinson research institute HTS wire critical current database," 2022 [Online]. Available: https://htsdb.wimbush.eu/dataset/4256624

[22] C. Senatore, C. Barth, M. Bonura, M. Kulich, and G. Mondonico, "Field and temperature scaling of the critical current density in commercial REBCO coated conductors," *Supercond. Sci. Technol.*, vol. 29, 2016, Art. no. 014002.

[23] "Finite element method magnetics. Documentation," 2022. [Online]. Available: https://www.femm.info/wiki/Documentation